Interactions between Poly(*N*-vinylformamide) and Sodium Dodecyl Sulfate As Studied by Fluorescence and Two-Dimensional NOE NMR Spectroscopy

Jung-Kai Tzeng and Sheng-Shu Hou*

Department of Chemical Engineering, National Cheng Kung University, Tainan 70101, Taiwan

Received October 16, 2007; Revised Manuscript Received December 3, 2007

ABSTRACT: The interaction of poly(*N*-vinylformamide) (PNVF) with anionic surfactant, sodium dodecyl sulfate (SDS), has been studied by pyrene fluorescence and two-dimensional nuclear Overhauser effect spectroscopy (2D NOESY). With use of pyrene as the probe, from low to high concentration of SDS, the pyrene I_1/I_3 plot exhibits three stages of association of PNVF with SDS. The I_1/I_3 plot vs [SDS] shows a well-defined plateau ($I_1/I_3 = 1.47$) at SDS concentrations ranging between 3 and 10 mM, indicating that in this range of SDS concentrations the sizes of polymer-bound SDS aggregates are approximately identical. The ambiguity in determining the critical aggregation concentration (cac) of SDS from the I_1/I_3 plot vs [SDS], which resembles the typical profile of surface tension vs surfactant concentration, has been clarified by the 2D NOESY experiment. Also, just beyond the cac ([SDS] = 3 mM), definite proof of formation of the PNVF−SDS complex bound on the polymer chain is provided by the 2D NOESY experiments. On the basis of the inter- and intramolecular cross-relaxation between the protons of PNVF and SDS, the microstructure of PNVF-induced SDS aggregates is proposed. Moreover, the association behavior of PNVF with SDS is compared to that of the poly(vinylpyrrolidone) (PVP)/SDS and poly(ethylene oxide) (PEO)/SDS systems.

Introduction

Interactions between water-soluble synthetic polymers and surfactants have been extensively explored for more than four decades. Researches on mixed polymer/surfactant systems have received increasing interest in the past few years because, on one hand, many current and promising applications grow in pharmaceutical formulations, food products, detergency, paints and inks, enhanced oil recovery, etc.,[1] and, on the other, the nature of association between the polymer and surfactant, especially at a concentration far below the critical micelle concentration (cmc) of the surfactant, remains equivocal.

Recently, *N*-vinylformamide (NVF) has been able to be produced in commercial scale quantities.[2,3] NVF-based polymers are regarded as the likely substitutes for polymers made from acrylamide, which is now widely known as a potential carcinogen. NVF is readily polymerizable and copolymerizable with other acrylic monomers to high polymers through traditional free radical polymerization.[4,5] Besides, basic or acidic hydrolysis of PNVF is the most convenient way for synthesizing poly(vinylamine).[6] New applications of NVF-based materials in many industrial fields are developing: for instance, inorganic oxide hybrid materials, papermaking, coating slips, petroleum recovery, hair care, and the drag reducing polymer.[5,7−10] Moreover, fundamental researches on NVF chemistry are of considerable recent interest.[6,11−13] To our knowledge, the interaction between PNVF and the widely used anionic surfactant, SDS, has not yet been studied.

One of the most significant aspects of the polymer/surfactant mixture is that the surfactant molecules form micelle-like aggregates at a well-defined concentration, often termed the critical aggregate concentration (cac). For systems of the nonionic polymer/ionic surfactant, the cac normally can be up to 1 order of magnitude lower than the normal cmc of the surfactant. At the cac, one often refers to that at which the polymer and surfactant start to interact; in other words, the onset of the association of polymer-bound surfactant molecules to form finite aggregates upon interacting with the polymer chains. Several complexation models for the polymer−surfactant aggregate have been brought up. For the mixed solution consisting of the ionic surfactant and uncharged homopolymer, the most quoted is the bead-necklace model.[14−16] It depicts that the surfactant molecules form discrete micellar-like aggregates along the polymer chain. Furthermore, there are two possible bead-necklace structures: the first is that the polymer chain wraps around the surface of the beads, i.e., the surfactant aggregates; the other structure represents the surfactant aggregates nucleating on the polymer chain, which penetrates through the surfactant aggregates.

Fluorescence emission of the fluorescent probes is a simple yet powerful technique for studying the interaction of polymer with surfactant. The applications of using fluorescent probes to study polymer/surfactant systems have been summarized in the excellent reviews.[17,18] The most often used hydrophobic probe is pyrene. The intensity ratio (I_1/I_3) of monomeric pyrene emission at 374 and 385 nm is proportional to microenvironment polarity. The smaller the I_1/I_3 value, the greater the increase in hydrophobicity of the environment where pyrene molecules locate. By plotting the I_1/I_3 ratio as a function of the surfactant concentration, the cmc of the surfactant itself or the cac of the surfactant in the presence of polymer can be determined. In addition to the monomeric emission, the broad and unstructured emission band maximum at 470 nm arises from the pyrene excimers, the complexes composed of an excited monomer and a ground-state pyrene. The intensity ratio between the excimer (I_E) and monomer emission (I_M) reflects local concentration of pyrene in a hydrophobic core.

The two-dimensional nuclear Overhauser effect spectroscopy (2D NOESY) experiment has been proved to be effective for providing insight into molecular features of surfactant micelles and mixed polymer−surfactant complexes.[19−28] 2D NOESY can

* To whom correspondence should be addressed. Tel: +886-6-2757575 ext 62641. Fax: +886-6-2344496. E-mail: sshou@mail.ncku.edu.tw.

10.1021/ma702296h CCC: $40.75
Published on Web 01/10/2008

reveal information about internuclear distances ($^1H-^1H$ in the present study) and hence proximity of the surfactant and polymer. In an early study using the NMR paramagnetic relaxation method, Gao et al. have indicated that PEO is located inside the SDS micelle.[29] Gjerde et al.[20] explicitly showed, by means of 2D NOESY, that poly(ethylene oxide) (PEO) penetrates into the interior of the SDS micelles because of the presence of NOE cross-peaks between PEO and SDS alkyl protons. Paduano and co-workers[26] studied the complex composed of poly(vinylpyrrolidone) (PVP) and sodium decyl sulfate (C10OS) and found no NOE between the terminal methyl protons of C10OS and the protons of PVP; thus, they concluded that the penetration of PVP in the C10OS aggregate is not so deep and that only the hydrophobic part of the ring enters slightly the core region. Nevertheless, the above studies were performed at a surfactant concentration much higher than the cmc of the surfactant. At a surfactant concentration higher than the cac but lower than its normal cmc, little is known about the microstructure of the surfactant aggregate and the association behavior of polymer and surfactant. Yuan et al.[25] reported that SDS molecules in the presence of poly(ethylene oxide) (PEO) self-aggregate but far removed from the polymer chain with [SDS], from the cac to the cmc. The alkyl protons of SDS are not in close contact (<0.5 nm) with the PEO protons until [SDS] is above the normal cmc of SDS (ca. 8.3 mM). Some arguments are still pending. Is this a general feature for all the nonionic polymer/anionic surfactant systems? If not, are the surfactant molecules, just beyond the cac, actually bound on the polymer chain via the short-range interaction (<0.5 nm), or do they only self-aggregate in the distant vicinity of the polymer chain? What is the microstructure of the polymer-induced surfactant aggregate at such low concentration of the surfactant?

In the present study, we are in focus on the interaction between water-soluble and uncharged PNVF and the anionic surfactant SDS, as studied by pyrene fluorescence and the 2D NOESY experiments. Furthermore, this paper aims at correlating the bulk solution properties obtained from pyrene fluorescence with, on the molecular level, the cooperative association behavior of surfactant to the polymer chain. The latter information could be provided by the 2D NOESY experiments. Finally, we compare the association behavior of the PNVF/SDS system with that of the PVP/SDS, PEO/SDS, and poly(*N*-isopropylacrylamide) (PNIPAMM)/SDS systems, which have been extensively investigated.

Experimental Section

Materials. Sodium dodecyl sulfate (SDS, Aldrich, 99%) and pyrene (Merck, >97%) were recrystallized from methanol prior to use. Cetylpyridinium chloride (CPC, Aldrich, 99%) and α,α′-azoisobutyronitrile (AIBN, Aldrich, 98%) were used as received. *N*-Vinylformamide (NVF, Aldrich, 98%) was purified by distillation under reduced pressure prior to use.

Synthesis of Poly(*N*-vinylformamide). Poly(*N*-vinylformamide) (PNVF) was prepared by the precipitation polymerization of NVF using AIBN as the initiator in toluene.[11,30] The polymerization was carried out in a four-necked 500 mL reactor at 60 °C for 24 h. The crude polymer was filtered and dissolved in water and then was purified by acetone/water reprecipitation repeatedly. The purified polymer was dried in a vacuum oven at 70 °C. The intrinsic viscosity of synthesized PNVF was 0.128 L/g, which was determined by an Ostwald viscometer at 35 °C. The number-average (M_n = 37 500) and weight-average molecular weight (M_w = 101 200) were obtained by SEC calibration with poly(ethylene oxide) standards in deionized water at 35 °C. The M_w was corrected with the universal calibration method using the Mark−Houwink relationship,[12] and the corrected M_w was 88 000. The overlap concentration (c^*) of PNVF in water is the reciprocal of the intrinsic viscosity, and the c^* equals 7.81 g/L. The concentrations of the polymer solutions studied in the present work are 3 and 5 g/L, which are below the c^*.

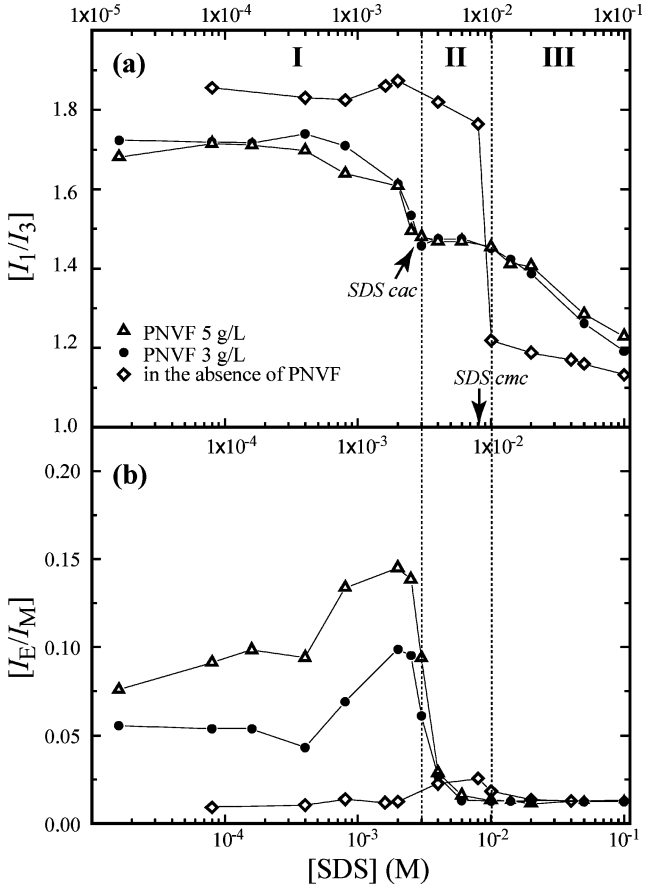

Figure 1. Plots of I_1/I_3 (a) and I_E/I_M (b) of pyrene solubilized in water (◇), 3 g/L PNVF (△), and 5 g/L PNVF (●) aqueous solutions as a function of SDS concentration. The cac of SDS (ca. 3 mM) in the presence of PNVF is taken as the onset of the plateau in region II.

Preparation of Solution Containing Pyrene for Spectroscopic Analysis. Pyrene-saturated aqueous solutions were prepared as follows: 2.5 mg of pyrene was added into 500 mL of Milli-Q water. After this solution was stirred for more than 24 h at room temperature in the dark, insoluble pyrene was removed by filtration. Increasing amounts of surfactant/pyrene-saturated solution (20 mL) were mixed with the PNVF/pyrene-saturated solutions (5 mL, PNVF concentration; [PNVF] = 15.0 or 25.0 g/L). All the samples were kept at room temperature in the dark for 24 h before measurements. The pyrene concentration was ca. 1.0×10^{-6} M in all samples for analysis.

Fluorescence Measurements. The fluorescence measurements were carried out on a F2500 spectrofluorometer (HITACHI). For experiments with pyrene, slit widths were set at 10 nm (excitation) and 2.5 nm (emission), and the excitation wavelength was 332 nm. The I_1/I_3 ratio was calculated as the ratio of peak I (374 nm) and peak III (385 nm) in the vibration fine structure of pyrene monomer emission. The I_E/I_M ratio was calculated as the ratio of the excimer emission intensity (I_E) at 470 nm and the intensity of peak I.

NMR Measurements. All NMR experiments were performed on a Bruker Avance-500 spectrometer at a proton resonance frequency of 500.13 MHz. The proton chemical shifts were referenced to the HOD signal at 4.70 ppm. The 2D NOESY spectra were acquired with the standard pulse program (90°−t_1−90°−t_m−90°−acquisition) of the Avance-500 spectrometer. For each NOE spectrum, 256 slices were recorded in the t_1 dimension, and the number of scans was 32 (2048 data points for each scan). The FID was treated by square-shifted sine bell weighting functions in both dimensions.

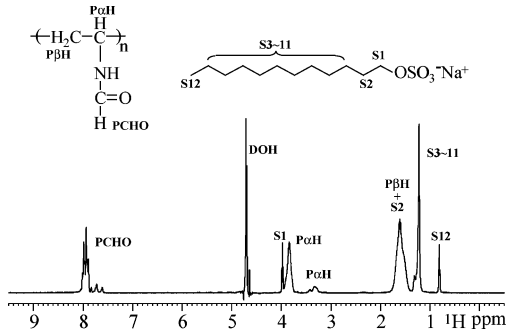

Figure 2. ^{1}H spectra and assignments of proton chemical shifts for the PNVF/SDS/D_2O solution. PαH and PβH denote the backbone methylene and methine protons of PNVF, and PCHO represents the aldehyde proton. Note that the chemical shift of S2 protons overlaps with that of PβH.

Results and Discussion

Pyrene Fluorescence of the PNVF/SDS System. The plots of pyrene I_1/I_3 and I_E/I_M ratios vs SDS concentrations at different PNVF concentrations are shown in Figure 1. In the absence of PNVF (open rhombuses), the cmc of SDS from the I_1/I_3 plot is found as ca. 8 mM. Above the cmc of SDS, the I_1/I_3 values are between 1.1 and 1.2. The results are in agreement with the reported literature values obtained by I_1/I_3 curve of pyrene.[31−33] The I_E/I_M ratios for SDS alone solution in Figure 1b can provide information on the distribution of pyrene molecules in the SDS solutions.[16,34] As SDS concentrations are lower than the cmc of SDS, the I_E/I_M ratios take low values ($\approx$0.011) and do not vary with SDS concentrations. Just above the cmc of SDS, pyrene molecules are solubilized in the SDS micelles, and hence the highest I_E/I_M ratio ($\approx$0.025) is observed as a result of the higher pyrene concentration in the SDS micelles. Further addition of SDS into the solution drastically increases the number of SDS micelles, but the total pyrene concentration in the solution is kept the same ([pyrene] $\approx 1.0 \times 10^{-6}$ M); therefore, pyrene molecules are compartmentalized in a large amount of micelles, and the I_E/I_M ratios drop to the low values again.

More complicated is the dependence of the I_1/I_3 and I_E/I_M plots on SDS concentrations for the 3.0 g/L (black circles) and 5.0 g/L PNVF (open triangles) solutions, as shown in Figure 1. The I_1/I_3 plots for the PNVF/SDS solutions can be subdivided into three distinct regions as indicated. In region I, at low SDS concentrations, the I_1/I_3 ratio remains independent of the surfactant concentration and is equal to ca. 1.7. The I_1/I_3 ratio starts to decrease slowly at [SDS] higher than 0.4 mM. The I_E/I_M ratios for the 5 g/L PNVF solution are between 0.075 and 0.095, which are higher than those ($\sim$0.050) of the 3 g/L PNVF solution. As compared to that of the pure SDS solution, the PNVF/SDS solutions exhibit lower I_1/I_3 ratios but higher I_E/I_M ratios, showing that the dissolved PNVF chains form the microdomains which are less polar than the bulk water phase. Note that the I_E/I_M ratio for the PNVF/SDS solution is significantly larger than that for the pure SDS solution at the cmc of SDS. It indicates that more pyrene molecules can be solubilized into the polymer coils than into the polymer-free SDS micelles.

With continuously increasing SDS concentration, the I_1/I_3 ratio goes to another well-defined plateau value (region II). This I_1/I_3 plateau spans from [SDS] = 3 to 10 mM, and its value is ca. 1.47. Correspondingly, the I_E/I_M plot in region II reveals that the I_E/I_M ratios drop drastically from the peak value to zero. This implies that a large amount of SDS aggregates formed upon adding more SDS into the system. On the other hand, in region II the invariant I_1/I_3 ratio indicates that the SDS aggregates formed have the same micropolarity. On the basis of the above results, it is reasonable to presume that SDS aggregates have the similar size through region II, and the number of SDS aggregates is increasing with increasing [SDS].

For the study of polymer/surfactant systems using pyrene as the probe, the cac was considered as the onset of formation of surfactant aggregates which host pyrene molecules. The I_1/I_3 curve for the studied PNVF/SDS system looks like the typical profile of surface tension vs surfactant concentration. The well-studied PVP/SDS system exhibits such kind of I_1/I_3 curve.[31] For the PVP/SDS system, the onset SDS concentration of the plateau is found in agreement with the generally accepted cac obtained from other techniques, though the first drop of the I_1/I_3 value starts at a very low SDS concentration (ca. 1 mM). Likewise, in the present study of the PNVF/SDS system, the inflection point of the I_1/I_3 plot between region I and region II, i.e., the onset of the plateau, is denoted as the cac. The applicability for taking the surfactant concentration at the onset of the plateau as the cac, rather than the first drop of the I_1/I_3 ratios, will be explored in terms of 2D NOESY experiments.

Past the plateau, in region III ([SDS] > 10 mM), I_1/I_3 ratio decreases slowly from the plateau value and lowers to ca. 1.2 at [SDS] = 0.1 M. However, at each fixed SDS concentration the I_1/I_3 ratio of the PNVF/SDS mixture in region III is larger than that of the pure SDS solution, showing that the structure of SDS micelles is looser by the presence of PNVF. It further suggests that the polymer chains penetrate into the micelles. Moreover, above the SDS cmc, PNVF−SDS complexes (more hydrophilic) and free SDS micelles (more hydrophobic) coexist;

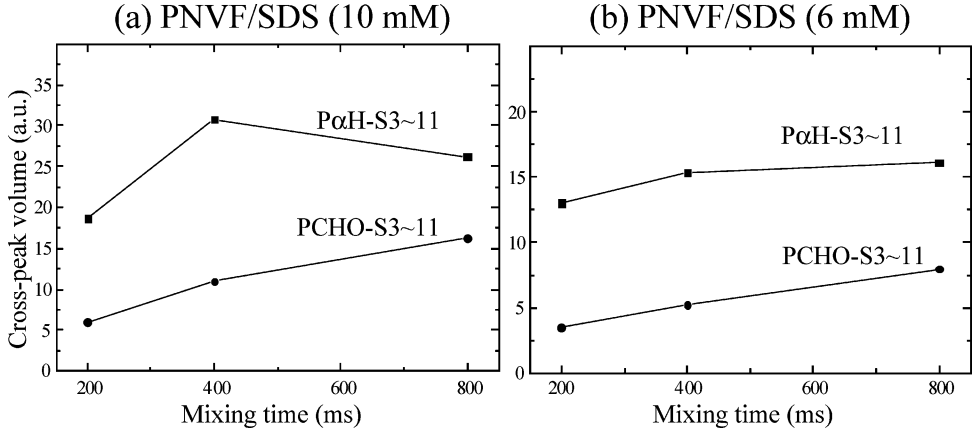

Figure 3. Buildup curve of cross-peak volume of PαH-S3$\sim$11 and PCHO-S3$\sim$11 with increasing mixing time. The SDS concentrations are 10 mM (a) and 6 mM (b). The cross-peak volume of PCHO-S3$\sim$11 increases approximately linearly with the mixing time.

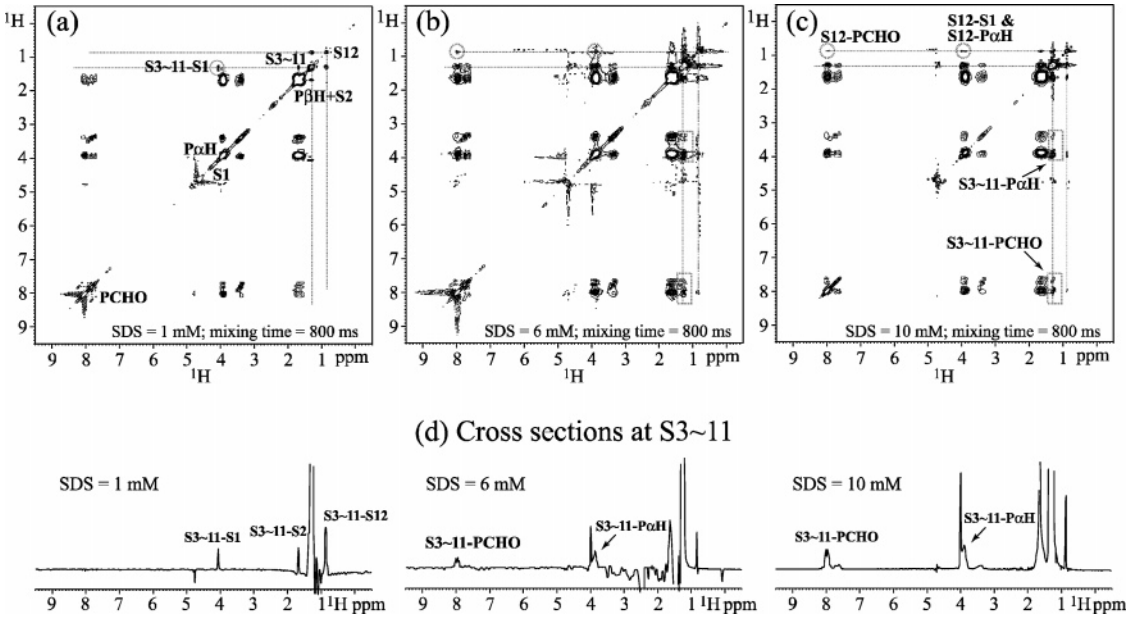

Figure 4. $^1H-^1H$ two-dimensional NOESY spectra for the PNVF/SDS/D_2O solutions at 1 mM (a), 6 mM (b), and 10 mM (c) of SDS. The mixing time is 800 ms, and the contour levels in the spectra are linearly spaced. The cross-peaks are in phase with the diagonal peaks. (d) The cross section taken at S3~11 along the ω_2 from each 2D spectrum. The cross-peaks shown in the 2D spectra and 1D cross sections clearly indicate that alkyl protons of SDS are in close contact (<0.5 nm) with polymer chains.

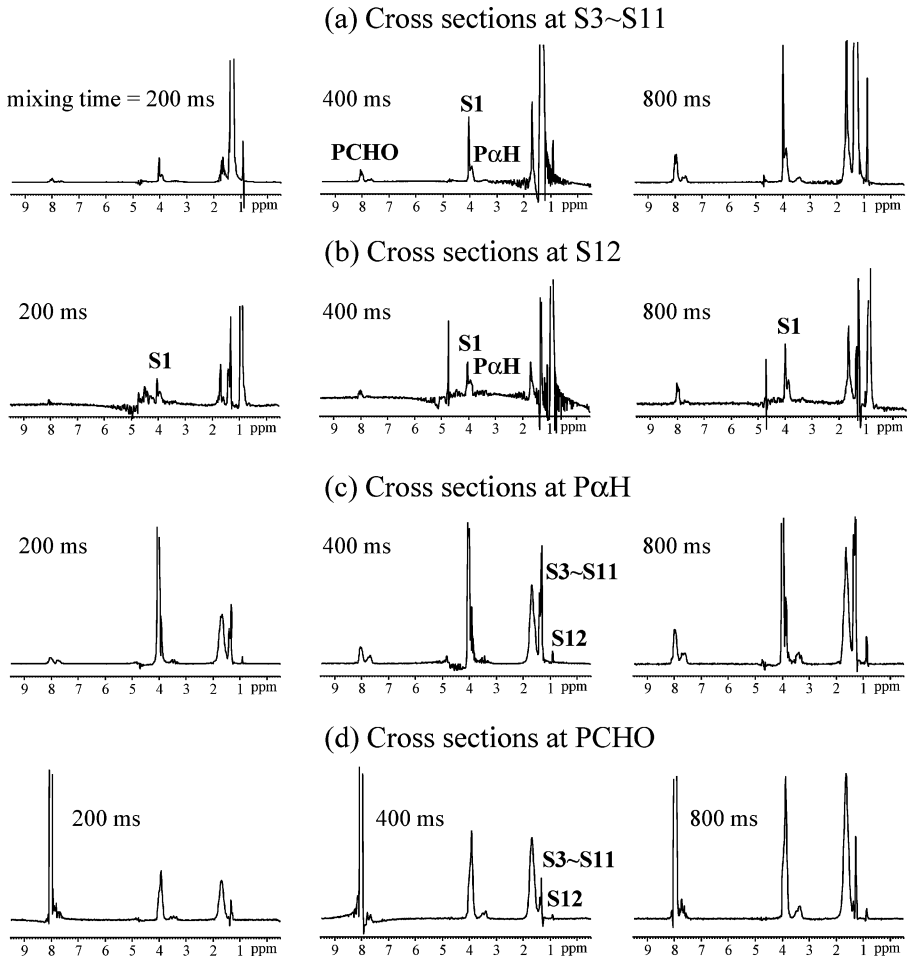

Figure 5. Cross sections along ω_2 taken at the position of S3~11, S12, PαH, and PCHO in the 2D NOESY spectra for the PNVF/SDS solution with [SDS] = 10 mM at different mixing times. Note that in (b) S12 is cross related with S1 even at t_m = 200 ms, indicating that S12 and S1 protons interact in proximity.

therefore, as the SDS-free micelle concentration increases, pyrene molecules will be distributed between the two environments, resulting in a gradual lowering of I_1/I_3 ratio.

Evidence of Short-Range Interaction between PNVF and SDS by 2D NOESY. The plot of pyrene I_1/I_3 vs [SDS] shows that, in the presence of PNVF, SDS molecules start to form

aggregates at [SDS] = 3 mM. However, in terms of pyrene fluorescence, it cannot tell whether the SDS aggregates are bound onto the polymer chains at such low SDS concentration. This question can be tackled by the 2D NOESY experiment.

The one-dimensional ^{1}H spectra and assignments of chemical shifts for the PNVF/SDS/D_2O mixture are shown in Figure 2. The isotope effect on the aggregation properties of most nonionic polymer/surfactant systems will not affect the experimental results and can be neglected.[35] It should be noted that PαH has two chemical shifts (δ = 3.83 and 3.32 ppm), and PCHO (the aldehyde proton) shows a complex pattern, rather than a single absorption peak. This is a consequence of polymerization of two NVF stereoisomers. The chemical shifts of PβH and S2 of SDS are overlapped; therefore, for the following 2D NOESY spectra the cross-relaxation between PNVF and SDS will be focused on the proton pairs of PαH-S3∼11, PαH-S12, PCHO-S3∼11, and PCHO-S12.

The cross-peaks of two specific protons of macromolecules shown in the 2D NOESY spectrum at a sufficiently short mixing time (t_m) means that they are close within a distance of 0.5 nm. However, except for the direct dipole−dipole interaction, indirect magnetization transfer due to spin diffusion also gives rise to cross-peaks between adjacent protons in the 2D NOESY spectrum. Spin diffusion occurs mainly for larger molecules and for long mixing times outside the initial rate regime, i.e., "linear approximation".[36] In general, spin diffusion will result in deceptive cross-peaks and incorrect conclusion on distances between two protons. In order to clarify the cross-peaks between SDS and PNVF are originated in primary NOE, the NOE buildup curve of the cross-peaks for the 5 g/L PNVF solution with [SDS] = 6 and 10 mM at three mixing times is shown in Figure 3. Similar to the other polymer/surfactant systems,[20,26,27] the PNVF/SDS system shows a slow buildup of intermolecular NOE. The cross-peak volume of PCHO-S3∼11 at t_m < 800 ms is approximately linearly dependent on the mixing times. Thus, the presence of cross-peaks S3∼11-PCHO at t_m smaller than 800 ms can be ascribed mostly to primary NOE. However, the cross-peak volume due to PαH-S3∼11 at t_m = 800 ms is reduced to or below the value of t_m = 400 ms. The different buildup behavior indicates that PCHO is in the proximity of the alkyl chain of SDS, whereas backbone protons (PαH) are out of the distance for which only primary NOE can occur. This is reasonable considering the PCHO protons are on the polymer side chain and thus can reach the alkyl protons first.

Figure 4a−c shows the 2D NOESY spectra (t_m = 800 ms) of the 5 g/L PNVF solution with [SDS] = 1, 6, and 10 mM, respectively. The proton spectrum (Figure 4d) shown under each 2D spectrum is the cross section in the ω_2 dimension taken at the peak of S3∼11. No cross-peak between SDS and PNVF is seen in Figure 4a, indicating that at [SDS] = 1 mM, which corresponds to the midpoint of the first I_1/I_3 reduction in region I, the SDS molecules are not in close contact (within 0.5 nm) with the polymer chains. While in region I the slow reduction in the I_1/I_3 ratios, beginning at [SDS] ≅ 1 mM, points to the possibility of formation of SDS aggregates, the 2D NOESY experiment shows that the SDS molecules are not bound on the polymer chains. It means that the lowering of the I_1/I_3, at the extremely low [SDS] (∼1 mM), is not necessarily an indication of a complex formation between the polymer and surfactant. As mentioned in the earlier discussion, a similar phenomenon has been observed for the PVP/SDS system.[31] There is still no proper explanation for the reduction in the I_1/I_3 ratio, starting at [SDS] below the accepted cac.[37]

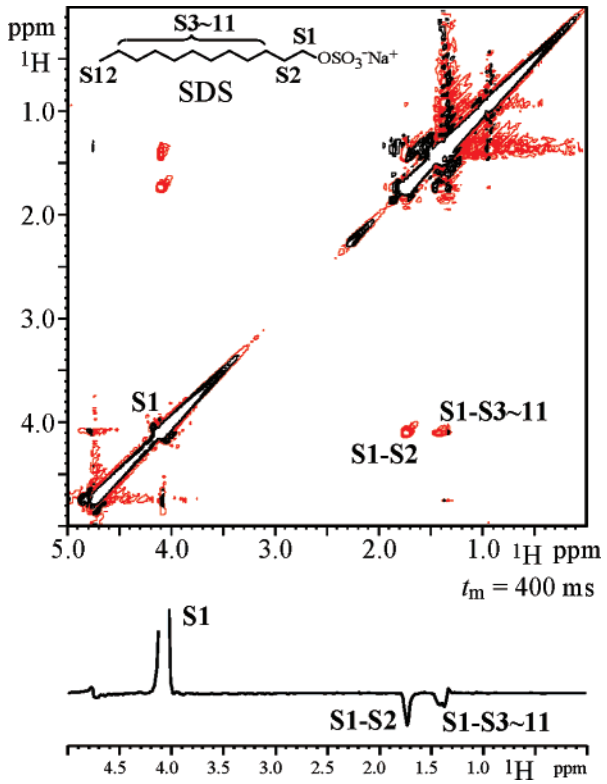

Figure 6. 2D NOESY spectrum of the pure SDS solution (15 mM). The 1D spectrum is the cross section taken at S1 along the ω_2. The mixing time is 400 ms, and the contour levels in the spectra are linearly spaced. The diagonal peaks are positive (in black), whereas the cross-peaks are negative (in red). No cross-peak between S1 and S12 is found.

In Figure 4b,c substantial cross-peaks between SDS protons (S12 and S3∼11) and PNVF protons (PCHO and PαH) are observed. The NOE cross-peaks confirm the fact that the SDS molecules are associated with polymer chains at [SDS] = 6 and 10 mM SDS, which corresponds the midpoint and endpoint of the I_1/I_3 plateau in region II. Since the experiments were performed under identical conditions, the intensity of the cross-peak reflects the number of protons associated with the polymer chains. Provided that the intensity of S3∼11 peak is normalized, in the cross sections taken at S3∼11 for [SDS] = 6 and 10 mM, the intensity of S3∼11-PCHO cross-peak increases proportionally with the SDS concentration. The result gives further evidence, which has been deduced from pyrene fluorescence, that in region II the number of SDS aggregates along the polymer chains increases as the SDS concentration is increased.

Structure of SDS Aggregates Bound on the Polymer Chains. Figure 5a−d shows the cross sections along ω_2 taken at the position of S3∼11, S12, PαH, and PCHO in the 2D NOESY spectra for the PNVF/SDS solution with [SDS] = 10 mM at different mixing times. At t_m = 200 ms the cross sections at S3∼11 and PαH reveal small, but clear, cross-peaks between SDS (S3∼11 and S12) and PNVF (PCHO and PαH), indicating that the alkyl chain of SDS molecules is unambiguously in close contact (<0.5 nm) with polymer chains. The result also supports that the polymer chains penetrate deeply through the interior of SDS aggregates. Unfortunately, the lack of resolution of the S3∼11 protons prohibits the identification of which protons of the alkyl chain are within a distance smaller than 0.5 nm from the polymer chains. In addition, in Figure 5c,d, the absence of the cross-peaks between the polymer protons (PCHO and PαH) and S1 (methylene protons next to the sulfate group) suggests that the sulfate group is distant from the polymer chain.

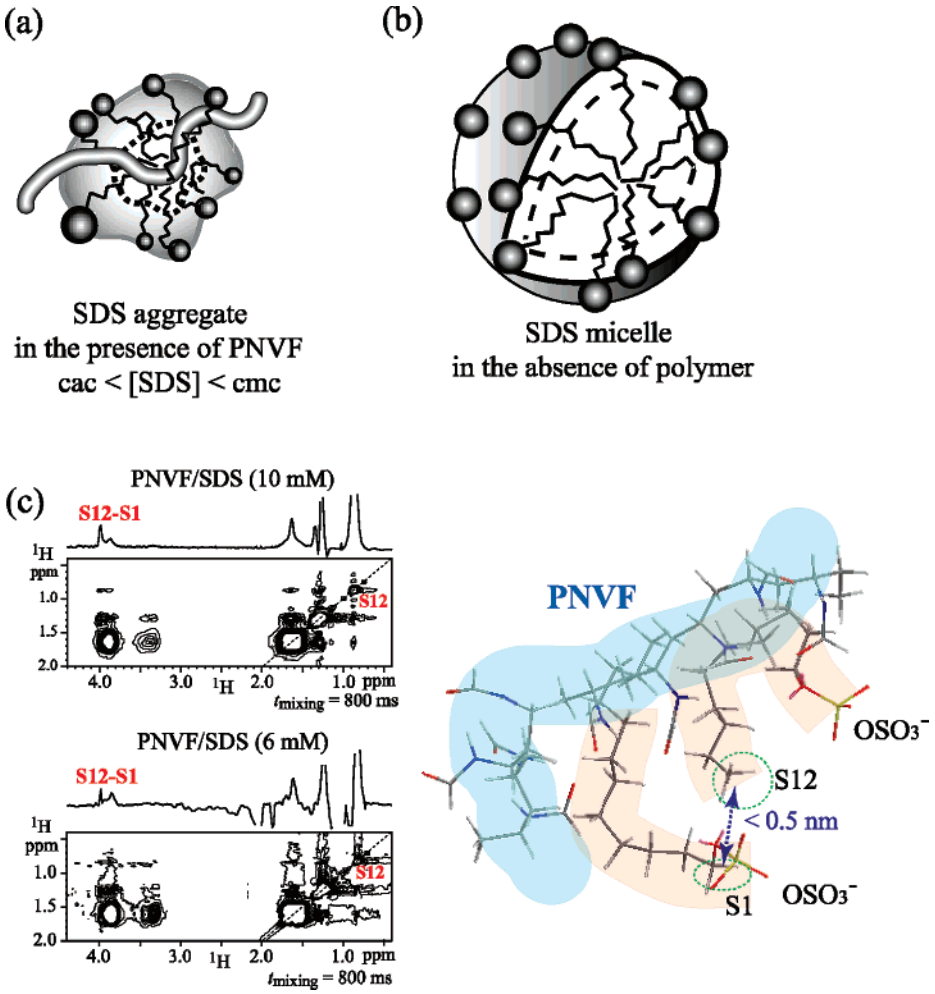

Figure 7. (a) An illustration of the complex structure of PNVF-induced SDS aggregate. The SDS alkyl chain is highly curled and partially associated with the polymer chain. The sulfate group is away from the polymer chain and exposed to water. Some SDS molecules protrude into the bulk water phase and some with more curled alkyl chains are closer to the polymer chain. (b) An illustration of the structure of a spherical SDS micelle. (c) Visualization of the possible structure (right) of surfactant molecules in the vicinity of the PNVF as deduced from the cross-relaxation effects in the 2D NOESY spectra (left). The 1D spectrum above the 2D spectrum is the cross section at S12 in the ω_2 dimension. The cross-peak between S12 and S1 is due to the intermolecular interaction of the SDS molecules.

It is worth noting that, even at the very short mixing time of 200 ms, a distinct cross-peak between S12 and S1 arises in the cross sections taken at S12 (as seen in Figure 5b). This S12−S1 cross-peak may be attributed to intra- or intermolecular interaction of the SDS molecules. However, if the intramolecular interaction really gives rise to the S12−S1 cross-peak, then the SDS molecules must possess an energetically unfavorable conformation. The alkyl carbons must be in the high-energy gauche positions so that the methyl group can bend and curve back to be close to the sulfate group. By excluding probability of intramolecular interaction, it is more rational that the intermolecular proximity causes the S12−S1 cross-peaks. In comparison, the 2D NOESY spectrum (Figure 6) for the pure SDS solution at [SDS] = 15 mM (>cmc) does not show the S12−S1 cross-peak at t_m = 400 ms. Thus, the conformation of SDS molecules in the polymer-free micelles certainly is different from that in the PNVF-induced SDS aggregates.

In Figure 7a, we propose the structure of SDS aggregates bound on the PVNF chains as deduced from the cross-relaxation results obtained by the 2D NOESY experiments. First of all, the SDS alkyl chain in the PNVF−SDS aggregate is in the more folded conformations, as compared to in the pure SDS micelle (Figure 7b). The sulfate group is away from the polymer chain because no correlation between S1 and polymer protons is seen in the 2D NOESY spectra. The curled alkyl chain of SDS is partially associated with the polymer chain. Because of the curled alkyl chain of SDS and perturbation from the polymer chain, we expect that the sulfate head groups are not closely packed and not forming a spherical surface, which is like that of the pure SDS micelle. Instead, the PNVF-induced SDS aggregate has a ragged interface with water; i.e., some SDS molecules protrude into the bulk water phase, and some with more curled alkyl chains are closer to the polymer chain. The molecular structure of PNVF−SDS complex shown in Figure 7c emphasizes that the folded conformation of SDS leads to the intermolecular cross relaxation between S12 and S1, which is observed in the 2D NOESY spectra ([SDS] = 6 and 10 mM).

The relative signs of the cross-peaks compared to the diagonal peaks in the 2D NOSEY spectrum are dependent on the correlation time, or motion, of the molecule under investigation. The NOE is positive for small molecules, and in the corresponding 2D spectrum the diagonal and cross-peaks have opposite sign. For macromolecules with slow molecular motion, the NOE is negative and the cross-peaks are in phase with the diagonal peaks. In Figure 6 ([SDS] = 15 mM), the SDS molecules exhibit positive NOE, indicating that the SDS molecules in the polymer-free micelle possess a rotational correlation time (τ_c) shorter than the critical correlation time ($\tau_{c,crit} = |\sqrt{5}/2\omega^0|$, ω^0 is the nuclear Larmor frequency in rad s^{-1}).[38] On the other hand, in all the NOESY spectra of the

PNVF/SDS mixtures the cross-peaks and diagonal peaks have the same sign. Therefore, the intermolecular NOE between PNVF and SDS as well as the intramolecular NOE of both PNVF and SDS are negative. It turns out that the SDS molecules have a τ_c longer than $\tau_{c,crit}$ as a result of being attached to the PNVF chains and tumbling together.

Comparison with Other Polymer/Surfactant Systems. The cac is a convenient measure of strength of the interaction between the polymer and surfactant. The lower cac represents stronger interaction between the polymer and surfactant. The following lists the cac, in decreasing strength of interaction, of several uncharged polymer/SDS systems which have been extensively studied:

$$\text{PNIPAAM (0.79 mM)}^{33} > \text{PVP (1.9 mM)}^{31,39} > \text{PNVF (3.0 mM)} > \text{PEO (4.2 mM)}^{40}$$

The greater hydrophobic character of PNIPAMM accounts for its extremely low cac (0.79 mM). The cac of the PNVF/SDS system is ca. 3 mM, which is slightly higher than that of the PVP/SDS system. Goddard[37] and Tedeschi et al.[41] have pointed out that the interaction of PVP with anionic surfactants originates in its weakly cationic character. On the basis of the results obtained from 2D NOESY and ^{13}C chemical shifts of the first methylene carbon of sodium decyl sulfate (C10OS), Roscigno et al.[26] concluded that the formation of C10OS−PVP complex was consequent on both hydrophobic interaction and electrostatic attraction. Considering the similarity in the chemical structure of PNVF and PVP, in both polymers the nitrogen atom is directly bonded to the backbone carbon and the carbonyl group. The difference is that PVP has ring methylenes on the polymer side chain, whereas PNVF bears only pendant aldehyde groups. Thus, the hydrophobic interaction of PVP with SDS presumably is stronger than the interaction between PNVF and SDS. This explains that the PNVF/SDS system has similar behavior of pyrene fluorescence and a higher cac, as compared to the PVP/SDS system.

It has been known that polyacrylamide (PAAm) shows no interaction with SDS[37] while the present study shows that PNVF strongly interacts with SDS. NVF and acrylamide are structural isomers, so the chemical structure of PNVF is analogous to that of PAAm. The major difference between them is that PNVF has dual functional groups, an amide and an aldehyde, whereas PAAm contains only the amide functional group. Therefore, this strong interaction between PNVF and SDS may be attributed to the aldehyde group, and it has been confirmed by the 2D NOESY experiments showing the cross-relaxation between the alkyl protons of SDS and the PNVF aldehyde group (see Figure 5d).

Experimental evidence[37] has shown that beyond the cac the surfactant molecules start to form micelle-like aggregates when interacting with the polymer. However, there are few direct proofs that confirm the surfactant aggregates really nucleate on the polymer chains, in particular at a concentration much lower than the cmc of the surfactant. For the PEO/SDS system the SDS molecules were found to be self-aggregated and far apart from the polymer chain at [SDS] between the cac and cmc.[25] On the contrary, the present study reveals that the PNVF-induced SDS aggregates are actually bound on the polymer chains at [SDS] just higher than the cac.

Conclusion

By means of pyrene fluorescence and 2D NOESY experiments, this study has confirmed that PNVF interacts strongly with SDS, though the repeat unit of PNVF is an isomer of that of PAAm which shows no interaction with SDS. According to the pyrene I_1/I_3 plot, association of SDS with PNVF against the amount of added SDS can be divided into three regions. In region I ([SDS] < 3 mM) no association of PNVF with SDS occurs. The 2D NOESY experiments show that at [SDS] = 1 mM there is no intermolecular cross-relaxation between the protons of PNVF and SDS. The result explains that the first drop of the I_1/I_3 ratio at the extremely low [SDS] does not mean complexation is taking place between of PNVF and SDS. In region II the I_1/I_3 ratio is independent of [SDS] (3 mM < [SDS] < 10 mM), and the cac of SDS (3 mM) is considered as the onset of the plateau. In addition, through region II the PNVF-induced SDS aggregates have the similar size, and the number of SDS aggregates increases with increasing [SDS]. Just beyond the cac, the SDS molecules start to nucleate on the PNVF chains forming the PNVF-bound aggregates; this is unlike the PEO/SDS system of which the SDS molecules are self-aggregated and far apart from PEO at [SDS] between the cac and cmc. The existence of cross-peaks between the terminal methyl protons (S12) and the PNVF protons indicates that the polymer chains penetrate deeply through the SDS aggregate. Moreover, the SDS molecule in the PNVF−SDS complex possesses a more curled conformation, as compared in the polymer-free SDS micelle. This results in the intermolecular cross-relaxation between the terminal methyl protons (S12) and the methylene protons (S1) next to the sulfate group, as seen in the 2D NOESY spectra. The microstructure of the PNVF−SDS complex is depicted and shown in Figure 7.

Acknowledgment. This work was supported by the National Science Council, Taiwan. We are very grateful to Ms. Ru-Rong Wu for her help in performing the NMR experiments.

References and Notes

(1) Goddard, E. D.; Ananthapadmanabhan, K. P. In *Polymer-Surfactant Systems*; Kwak, J. C. T., Ed.; Marcel Dekker: New York, 1998.
(2) Linhart, F.; Degen, H.; Auhorn, W.; Kroener, M.; Hartmann, H.; Heide, W. US Patent 4,772 359, 1988.
(3) Lai, T. Eur Patent Application 0264649, 1990.
(4) Kathmann, E. E. L.; McCormick, C. L. *Macromolecules* **1993**, *26*, 5249.
(5) Pinschmidt, R. K.; Wasowski, L. A. J.; Orphanides, G. G.; Yacoub, K. *Prog. Org. Coat.* **1996**, *27*, 209.
(6) Yamamoto, K.; Imamura, E.; Nagatomo, E. S., T.; Muraoka, Y.; Akashi, M. *J. Appl. Polym. Sci.* **2003**, *89*, 1277.
(7) Spange, S.; Meyer, T.; Vogit, I.; Eschner, M.; Estel, K.; Pleul, D.; Simon, F. *Adv. Polym. Sci.* **2004**, *165*, 43.
(8) Wang, F.; Takana, H. *J. Appl. Polym. Sci.* **2000**, *78*, 1805.
(9) Marhefka, J. N.; Marascalco, P. J.; Chapman, T. M.; Russell, A. J.; Kameneva, M. V. *Biomacromolecules* **2006**, 1597.
(10) Senden, R. J.; De Jean, P.; McAuley, K. B.; Schreiner, L. J. *Phys. Med. Biol.* **2006**, *51*, 3301.
(11) Hong, J.; Pelton, R. *Colloid Polym. Sci.* **2002**, *280*, 203.
(12) Singley, E. J.; Daniel, A.; Person, D.; Beckman, E. J. *J. Polym. Sci., Part A: Polym. Chem.* **1997**, *35*, 2533.
(13) Kroner, M.; Dupis, M.; Winter, M. *J. Prakt. Chem.* **2000**, *342*, 115.
(14) Nagarajan, R.; Kalpakci, B. *Polym. Prepr.* (*Am. Chem. Soc., Div. Polym. Chem.*) **1982**, *23*, 41.
(15) Nagarajan, R.; Kalpakci, B. In *Microdomains in polymer Solutions*; Dubin, P. L., Ed.; Plenum Press: New York, 1985; p 386.
(16) Turro, N. J.; Lei, X.-G. *Langmuir* **1995**, *11*, 2525.
(17) Winnik, F. M. In *Interactions of Surfactants with Polymers and Proteins*; Goddard, E. D., Ananthapadmanabhan, K. P., Eds.; CRC Press: Boca Raton, FL, 1992; pp 367−394.
(18) Winnik, F. M.; Regismond, S. T. A. *Colloids Surf., A* **1996**, *118*, 1.
(19) Zhao, J.; Fung, B. M. *J. Phys. Chem.* **1993**, *97*, 5187.
(20) Gjerde, M. I.; Nerdal, W.; Hoiland, H. *J. Colloid Interface Sci.* **1996**, *183*, 285.
(21) Kreke, P. J.; Magid, L. J.; Gee, J. C. *Langmuir* **1996**, *12*, 699.
(22) Yuan, H. Z.; Zhao, S.; Yu, J. Y.; Shen, L. F.; Du, Y. R. *Colloid Polym. Sci.* **1999**, *277*, 1026.
(23) Yuan, H. Z.; Cheng, G. Z.; Zhao, S.; Miao, X. J.; Yu, J. Y.; Shen, L. F.; Du, Y. R. *Langmuir* **2000**, *16*, 3030.

(24) Yuan, H. Z.; Miao, X. J.; Zhao, S.; Shen, L. F.; Yu, J. Y.; Du, Y. R. *Magn. Reson. Chem.* **2001**, *39*, 33.
(25) Yuan, H. Z.; Luo, L.; Zhang, L.; Zhao, S.; Mao, S. Z.; Yu, J. Y.; Shen, L. F.; Du, Y. R. *Colloid Polym. Sci.* **2002**, *280*, 479.
(26) Roscigno, P.; Asaro, F.; Pellizer, G.; Ortona, O.; Paduano, L. *Langmuir* **2003**, *19*, 9638.
(27) Roscigno, P.; D'Auria, G.; Falcigno, L.; D'Errico, G.; Paduano, L. *Langmuir* **2005**, *21*, 8123.
(28) Emin, S. M.; Denkova, P. S.; Papazova, K. I.; Dushkin, C. D.; Adachi, E. *J. Colloid Interface Sci.* **2007**, *305*, 133.
(29) Gao, Z.; Wasylishen, R. E.; Kwak, J. C. T. *J. Phys. Chem.* **1991**, *95*, 462.
(30) Badesso, R. J.; Lai, T. W.; Pinschmidt, R. K. J.; Sagal, D. J.; Vijayendran, B. R. *Polym. Prepr.* (*Am. Chem. Soc., Div. Polym. Chem.*) **1991**, *32*, 110.
(31) Turro, N. J.; Baretz, B. H.; Kuo, P. L. *Macromolecules* **1984**, *17*, 1321.
(32) Ananthapadmanabhan, K. P.; Goddard, E. D.; Turro, N. J.; Kuo, P. L. *Langmuir* **1985**, *1*, 352.
(33) Schild, H. G.; Tirrell, D. A. *Langmuir* **1991**, *7*, 665.
(34) Siu, H.; Duhamel, J. *Macromolecules* **2006**, *39*, 1144.
(35) Pettersson, E.; Topgaard, D.; Stilbs, P.; Söderman, O. *Langmuir* **2004**, *2004*, 1138.
(36) Cavanagh, J.; Fairbrother, W. J.; Palmer III, A. G.; Skelton, N. J. *Protein NMR Spectroscopy: Principles and Practice*; Academic Press: San Diego, CA, 1996.
(37) Goddard, E. D. *Colloids Surf.* **1986**, *19*, 255.
(38) Levitt, M. H. *Spin Dynamics: Basic of Nuclear Magnetic Resonance*; John Wiley & Sons Ltd.: West Sussex, UK, 2003.
(39) Shannigrahi, M.; Bagchi, S. *J. Phys. Chem. B* **2005**, *109*, 14567.
(40) Wang, G.; Olofsson, G. *J. Phys. Chem. B* **1998**, *102*, 9276.
(41) Tedeschi, A. M.; Busi, E.; Basosi, R.; Paduano, L.; D'Errico, G. *J. Solution Chem.* **2006**, *35*, 951.

MA702296H